

# Fitts' Law for speed-accuracy trade-off is a diversity sweet spot in sensorimotor control

Yorie Nakahira<sup>1,#</sup>, Quanying Liu<sup>1,#</sup>, Terrence J. Sejnowski<sup>2,3\*</sup>, John C. Doyle<sup>1\*</sup>

<sup>1</sup>Division of Engineering and Applied Science, California Institute of Technology,  
Pasadena, CA 91125, USA

<sup>2</sup>The Salk Institute for Biological Studies, La Jolla, CA, USA

<sup>3</sup>Division of Biological Sciences, University of California, San Diego, La Jolla, CA, USA

#These authors contributed equally

\*To whom correspondence should be addressed; E-mail: doyle@caltech.edu, terry@salk.edu.

**Human sensorimotor control exhibits remarkable speed and accuracy, as celebrated in Fitts' law for reaching. Much less studied is how this is possible despite being implemented by neurons and muscle components with severe speed-accuracy tradeoffs (SATs). Here we develop a theory that connects the SATs at the system and hardware levels, and use it to explain Fitts' law for reaching and related laws. These results show that *diversity* between hardware components can be exploited to achieve *both fast and accurate* control performance using slow or inaccurate hardware. Such “diversity sweet spots” (DSSs) are ubiquitous in biology and technology, and explain why large heterogeneities exist in biological and technical components and how both engineers and natural selection routinely evolve fast and accurate systems from imperfect hardware.**

Human sensorimotor control is remarkably fast and accurate despite being implemented using slow or inaccurate components (1–6). For example, Fitts’ Law predicts that, in many forms of reaching (e.g. eye gaze, hand, mouse), the time required for reaching quickly to a target of width  $W$  at distance  $D$  scales as  $\log_2(2D/W)$  (7, 8). The logarithmic relation between the reaching time and target width allows faster speed to be achieved with a small decrement in accuracy. On the other hand, the speed-accuracy tradeoffs (SATs) of the hardware implementing control can be much more severe. Improving either speed or accuracy in nerve signaling or muscle actuation requires profligate biological resources (6); as a consequence, only a few types of nerves and muscles are built to be both fast and accurate (Fig. 1). Such apparent discrepancy between the speed-accuracy tradeoffs in sensorimotor control and neurophysiology poses the question: how does nature deconstrain neurophysiological hardware constraints in sensorimotor control?

In this paper, we develop a networked control system model to relate the SATs in sensorimotor control and neurophysiology. The model characterizes how hardware SATs in nerves and muscles impose fundamental limits in sensorimotor control and recovers Fitts’ Law as a special case. The results show that appropriate speed-accuracy diversity at the level of neurons and muscles allow nervous systems to improve the speed and accuracy in control performance despite using slow or inaccurate hardware, which we call “Diversity Sweet Spots.”

We consider a feedback loop in Fig. 2A. Here, the error between the actual position and the desired position  $x(t+1)$  is computed from the previous error  $x(t)$ , the sensed uncertainty  $w(t)$ , and the control action  $u(t)$  as follows:

$$x(t+1) = x(t) + w(t) + u(t). \quad (1)$$

The control action, characterized by  $\mathcal{K}$ , is generated from the observed errors, sensed uncer-

tainty, and past control actions, *i.e.*

$$u(t + T) = \mathcal{K}(x(0 : t), w(0 : t - 1), u(0 : t + T - 1)). \quad (2)$$

using sensing components such as eyes and muscle sensors; communication components such as nerves; computing components such as the cortex in the central nervous system; and actuation components such as eye and arm muscles. The total delay from the disturbance to the control action is given by  $T := T_s + T_i$ , where  $T_s$  captures the latency in nerve signaling, and  $T_i$  captures other internal delays in the feedback loop. We constrain that the feedback loop can only transmit  $R$  bits of information per unit time (denote as signaling rate) (9). Table S1 in the Supplementary Material summarizes the above parameters.

The communication components, axons in sensory nerves or motor neurons, carry sensory information from the periphery into the brain and activate muscles in the final common pathway. There exist heterogeneity in the size and number of axons within a nerve bundle and between different types of sensory nerves, with calibers in mammals ranging over two orders of magnitude from tenths of microns to tens of microns (10–13). This size and number heterogeneity lead to extreme differences in neural signaling speed and accuracy as the speed and rate of information flow in an axon depend on its diameter and myelination. To quantify the bundle of axons in certain nerves, we model axon bundles as a communication channel with signaling delay  $T_s$  and signaling rate  $R$ . Building upon (6) and references therein, we show in the Supplementary Materials that, under some assumptions, the nerve signaling SAT can be modeled by

$$R = \lambda T_s. \quad (3)$$

where  $\lambda$  is proportional to the spatial and metabolic cost to build and maintain the nerves. The nerve signaling SATs differ from species to species and increase in animal size (13, 14). Eq. 3 can be refined or modified given specific types of nerves or encoding mechanisms, but the rest

of our framework does not require the component SATs to have any specific form. So for the rest of this paper, we use Eq. 3 to demonstrate how the SATs at the component level impact those at the system level.

The actuation components, muscle, also have tradeoffs in terms of the reaction speed, accuracy in strength level, maximum strength, and ease of fatigue. Moreover, most muscles carry diverse muscle fibers, *e.g.*, striated muscles typically have both large fast twitch fibers and many more smaller slow twitch muscles (Fig. 1B). In particular, its SATs can be modeled using a simplified muscle model that includes  $m$  motor units, indexed by  $i \in \{1, 2, \dots, m\}$ , each associated with a reaction speed and a fixed strength. We use  $F_i$  to denote its strength and assume without loss of generality that  $F_1 \leq F_2 \leq \dots \leq F_m$ . According to Henneman's size principle (15), motor units in the spinal cord are recruited in ascending order of  $F_i$ , so a muscle (at non-transient time) can only generate  $m + 1$  discrete strength levels:  $\sum_{i=1}^n F_i$ , where  $n$  can take any integer from 0 to  $m$ . Given a fixed length, the maximum strength of a muscle  $\ell = \sum_{i=1}^m F_i$  is known to be proportional to its cross-sectional area (16). This implies that, given a fixed space to build a muscle, its maximum strength does not depend on the specific composition of motor units. Constrained on the maximum strength, a muscle can be built from many motor units with small strengths or a few motor units with large strengths. In the former case, the muscle has better resolution but slower reaction speed, while in the latter case, the muscle has faster reaction speed but coarser resolution (see Fig. S2 in the Supplementary Material). This SAT can be quantified using the following formula:

$$\dot{a}_i(t) = \alpha f_i^p(t)(1 - a_i(t)) - \beta a_i(t) \quad a_i^q(t) = c_i(t) \quad (4)$$

where  $\alpha = 1, \beta = 1, p = 1, q = 3$  are fixed constants (17). If a motor unit is recruited at time  $t = 0$ , then its strength  $c_i(t)$  rises according to Eq. 4 with  $f_i(t) = 1(t)/((1/F_i)^{1/q} - 1)$ , where  $1(t)$  is a unit step function. Similarly, when a recruited motor unit is released at time  $t = \tau$ , its

contraction rate falls according to Eq. 4 with  $f_i(t) = 1(-t + \tau)/((1/F_i)^{1/q} - 1)$ . From Eq. 4, the reaction speed of a muscle is an increasing function of  $F_i$  (18), so better resolution (having small  $F_i$ ) can only be achieved with decreased reaction speed.

Next, we use the basic model (Eq. 1 and Eq. 2) to study how the nerve SATs impact the system SATs in reaching. In a reaching task, the subjects' goal is to move their hand or cursor to a target as rapidly and accurately as possible. This setting can be recovered by setting  $w(t) = d\delta(t)$  in Eq. 1, where  $d \in [-D, D]$  is the distance between the initial position and the target position, and  $\delta(t)$  is the Kronecker delta function (19). There exist tradeoffs between the reaching speed and accuracy, where the speed of reaching is quantified by the reaching time  $T_r$  (*i.e.* time taken to reach the target area), and the accuracy is quantified by normalized target width  $W/D$ . The relation between  $T_r$  and  $D/W$  satisfies

$$\sup_{|d| \leq D} T_r \geq T + \frac{1}{R} \log_2(2D/W). \quad (5)$$

This formula recovers Fitts' law (8, 20), which states that the reaching time follows  $T_r = p + q \log_2(2D/W)$ , where  $F := \log_2(2D/W)$  is called the Fitts' index of difficulty, and  $p$  and  $q$  are fixed constants. The proof of Eq. 5 can be found in the Supplementary Material, but its intuition can be obtained as follows: identifying a target of width  $W$  in range  $[-D, D]$  requires  $F$  bits of information, and transmitting  $F$  bits of information requires  $F/R$  time steps with additional  $T$  time steps of (transmission) delay in the feedback loop.

Eq. 5 decomposes into two terms: the term  $T$  that is only a function of the delay, and the term  $\frac{1}{R} \log_2(2D/W)$  that is only a function of the data rate. Therefore, we can consider the first term as the cost in reaching time due to having delay in the feedback loop (denote as the delay cost), and the second term as the cost due to having limited data rate in the feedback loop (denote as the rate cost). By combining the component-level SATs in Eq. 3 and the system-level SATs in Eq. 5, we can predict how the SATs in neural signaling impact sensorimotor control

in Fig. 3A. Eq. 5 suggests that the signaling delay  $T_s$  affects the reaching time  $T_r$  in a linear manner, whereas the signaling rate  $R$  affects  $T_r$  in an inversely proportional manner.

We tested these theoretical predictions with reaching experiments (Fig. 2B,C). The subjects were asked to control a steering wheel with added delays, quantization, and both (see the Supplementary Material for details), and their reaching times for each case are shown in Fig. 3B. Fig. 3 suggest that axon compositions that minimize either the signaling delay or the rate alone suffer from large delay or rate costs, rendering the system suboptimal. Conversely, the minimum reaching time is achieved when both the signaling delay and rate are chosen to be moderate levels, leading to a minimum delay plus rate costs. In particular, subject to the nerve SAT Eq. 3, the minimum reaching time is achieved at  $T = \sqrt{F/\lambda}$ ,  $R = \sqrt{\lambda F}$ . The optimal  $T$  and  $R$  is increasing/decreasing in  $F$ . This is because as the index of difficulty  $F$  increases, the reaching task requires more accuracy, and the data rate limit gains greater impact on the reaching time. Thus, for a reaching task with large  $F$ , fast reaching times are achieved with increased data rate  $R$  at the expense of increased delay  $T$ .

The dependencies of optimal nerve signaling speed and accuracy ( $T, R$ ) on  $F$  suggests that diversity in signaling speed and accuracy allows better reaching performance with a broad range of difficulties. Indeed, there exists heterogeneity in the size and number of axons within a nerve bundle and between different types of sensory nerves, with calibers in mammals ranging over two orders of magnitude from tenths of microns to tens of microns (11–13). As the speed and rate of information flow in an axon depend on its diameter and myelination (21, 22), this size and number heterogeneity lead to extreme differences in neural signaling speed and accuracy.

Eq. 5 assumes that the SATs in nerve signaling are the bottleneck in the reaching task. Although this assumption is valid for certain eye movements or small-distance reaching, in many other types of reaching tasks, muscle actuation SATs is the major limiting factors in the reaching SATs. To understand how the muscle SATs impact the reaching SATs, we model the

sensorimotor system by Eq. 1 and Eq. 2 with limited muscle actuation SATs, which is obtained from Eq. 4.

We compare the reaching SATs when the muscle (actuation component) contains uniform versus diverse motor units in Fig. 4A. Having diversity within muscles largely improves the reaching SATs because, when muscles are built from diverse motor units, large motor units allow for faster activation at the beginning of a reaching, while small motor units can be used to fine-tune the force toward the end of reaching. This benefit of diversity can also be found in the design of our arm, which combines large arm muscles and joints with small figures. This combination of fast coarse movements and slow fine ones is known to produce a logarithmic law (?), which possesses a sweet spot between in speed and accuracy.

We confirmed the benefit of diversity using reaching experiments (Figs. 2B,C,S5). In the experiments, subjects were asked to move to a target of fixed width as fast as possible under two settings: using uniform speed or diverse speeds. Fig. 4B compares their reaching SATs when only one level of speed was allowed versus when two levels of speed were allowed. The performance under diverse speed largely outperforms that under uniform speed. Moreover, a uniform speed gave rise to a linear SAT which is not consistent with the logarithmic form of Fitts' law, while the flexibility to use diverse speeds yielded a DSS like Fitts' law, in which fast reaching can be performed accurately. The logarithmic form of Fitts' law has been confirmed in many experiments and explained using various models (see (8, 20, 23–25) and references therein). Our results reveal that Fitts' law arises from DSSs, in which the hardware diversity is key for achieving fast and accurate performance using slow or inaccurate hardware. This relation of DSSs and logarithmic laws potentially provide new insights into other logarithmic laws observed (26).

DSSs may also help us understand how engineered systems can achieve fast and accurate performance with slow or inaccurate components. For example in a transportation system, no

single mover (*e.g.* walking, driving, flying) can rapidly take you from one point on the earth to another. But a combination of an airplane that rapidly takes you from one city to another, and ground transportation, which can take you more slowly from one part of a city to another, and walking, which can take you even more slowly from one point to another, can together achieve fast and accurate transport (see the Supplementary Material).

Although this paper focuses on the benefit of hardware diversity and its connection to Fitts law, DSSs can also be observed in the layered architectures used in different types of control, such as the control of eye movements (4, 5), and decision making in general (27–29). Take an example of our visual system, involving diverse control layers. The vestibulo-ocular reflex is a layer that performs fast but inaccurate negative feedback control to stabilize images on the retina against rapid head movements. This layer works in concert with another layer that performs smooth pursuit, a slow but accurate cortical system for tracking slowly moving visual objects. These two layers jointly create a virtual eye controller that is both fast and accurate. More detail about DSSs in layered control architectures, like the visual system, is presented in our companion paper (30). More generally, DSSs may reveal a more general design principle for distributed control in brains and inspire the design of large-scale technological systems.

## References and Notes

1. E. Todorov, M. I. Jordan, *Nature neuroscience* **5**, 1226 (2002).
2. A. J. Nagengast, D. A. Braun, D. M. Wolpert, *Journal of neurophysiology* **105**, 2668 (2011).
3. D. W. Franklin, D. M. Wolpert, *Neuron* **72**, 425 (2011).
4. S. Lac, J. L. Raymond, T. J. Sejnowski, S. G. Lisberger, *Annual review of neuroscience* **18**, 409 (1995).
5. S. G. Lisberger, *Neuron* **66**, 477 (2010).
6. P. Sterling, S. Laughlin, *Principles of neural design* (MIT Press, 2015).
7. P. M. Fitts, J. R. Peterson, *Journal of experimental psychology* **67**, 103 (1964).
8. Fitts's law (wikipedia).
9. A summary of the parameters used is given in **Table S1**.
10. J. A. Perge, J. E. Niven, E. Mugnaini, V. Balasubramanian, P. Sterling, *Journal of Neuroscience* **32**, 626 (2012).
11. J. Stenum, *Journal of Experimental Biology* **221**, jeb170233 (2018).
12. H. L. More, *et al.*, *Journal of Experimental Biology* **216**, 1003 (2013).
13. H. L. More, *et al.*, *Proceedings of the Royal Society B: Biological Sciences* **277**, 3563 (2010).
14. Bigger animals have more inertia and can tolerate longer delays. they also use more time to compute in part because large animals (elephants, etc.) are more prone to falling.

15. E. Henneman, G. Somjen, D. O. Carpenter, *Journal of neurophysiology* **28**, 560 (1965).
16. G. Goldspink, *Journal of experimental biology* **115**, 375 (1985).
17. V. Brezina, I. V. Orekhova, K. R. Weiss, *Journal of neurophysiology* **83**, 207 (2000).
18. In other words, the time required for a muscle to reach to  $c_i(t) = f_i$  from  $c_i(0) = 0$  is decreasing in  $f_i$ .
19. The Kronecker delta function is defined as follows:  $\delta(t) = 1$  if  $t = 0$ , and  $\delta(t) = 0$  otherwise.
20. P. M. Fitts, *Journal of experimental psychology* **47**, 381 (1954).
21. A. Hodgkin, *The Journal of physiology* **125**, 221 (1954).
22. D. Hartline, D. Colman, *Current Biology* **17**, R29 (2007).
23. T. O. Kvåiseth, *Perceptual and Motor Skills* **49**, 291 (1979).
24. I. S. MacKenzie, *Journal of motor behavior* **21**, 323 (1989).
25. H. Hatze, *Bulletin of mathematical biology* **41**, 407 (1979).
26. These laws include the weber-fechner law, a log relation between the physical change in a stimulus and the perceived change in human perception; the ricco law for visual target detection for unresolved targets; the accot-zhai law for steering, a generalization of fitts' law for 2d environments; the spacing effect of ebbinghaus for long-term recall from memory; and the hick-hyman law for the logarithmic increase in the time it takes to make a decision as the number of choices increases.
27. D. Kahneman, P. Egan, *Thinking, fast and slow*, vol. 1 (Farrar, Straus and Giroux New York, 2011).

28. N. R. Franks, A. Dornhaus, J. P. Fitzsimmons, M. Stevens, *Proceedings of the Royal Society of London. Series B: Biological Sciences* **270**, 2457 (2003).
29. L. Chittka, P. Skorupski, N. E. Raine, *Trends in ecology & evolution* **24**, 400 (2009).
30. Y. Nakahira, et. al, Diversity sweet spots in layered architectures and speed-accuracy trade-offs in sensorimotor control. Unpublished.

## **Acknowledgments**

This research was supported by National Science Foundation (NCS-FO 1735004 and 1735003). Q.L. was supported by a Boswell fellowship and a FWO postdoctoral fellowship (12P6719N LV).

## Figures

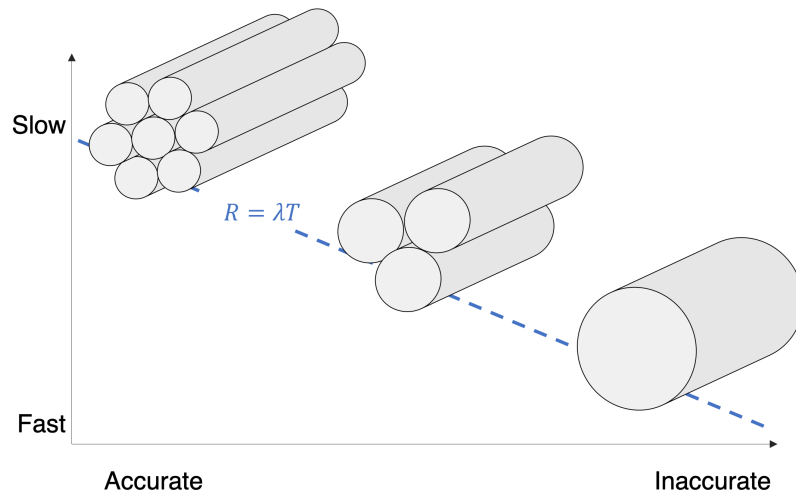
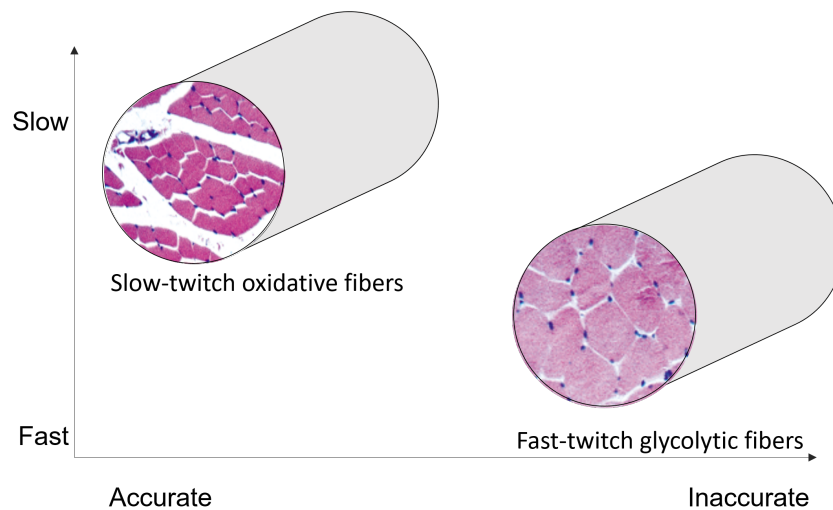
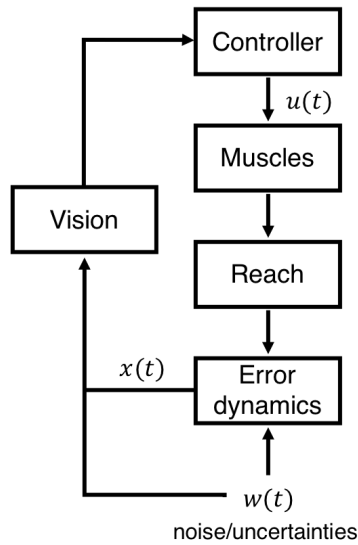
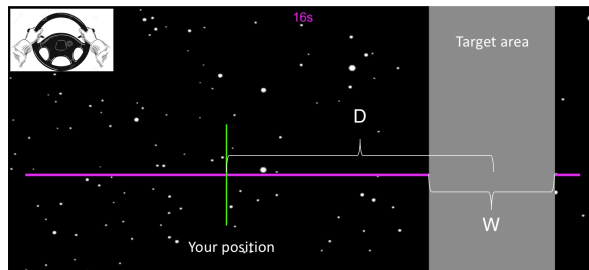
**A****B**

Figure 1: Component-level speed-accuracy trade-off (SAT) in nerves and muscles. (A) Cartoon diagram showing how nerve size and number trade-offs result in its signaling SATs. The region above the dashed line represents the achievable speed and accuracy given a fixed total cross-sectional area, which is proportional to  $\lambda$ . (B) Different types of muscle fibers and their resulting actuation SATs. The one with a smaller diameter and darker color (due to larger amounts of myoglobin, numerous mitochondria, and extensive capillary blood supply) are the oxidative fibers, and the other is the glycolytic fibers. Oxidative fibers are slower but more accurate, whereas glycolytic fibers are faster but less accurate.

A



B



C

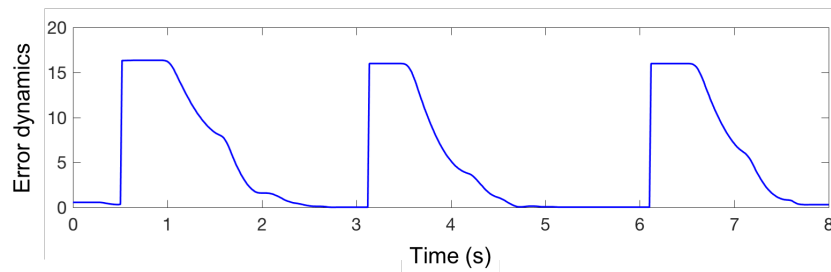


Figure 2: The model and system. (A) Block diagram of the sensorimotor control model that simulates the reaching task. Each box is a component in the model that communicates (vision), computes (controller), or actuates (muscles) with potentially limited speed and accuracy. (B) Video interface for the reaching experiment. The green line indicates the player's position and the gray zone is the target. The subjects' goal is to steer the wheel to reach the target as fast as possible and stay at the target. (C) An error dynamics measured in an experiment. The error  $x(t)$  is defined as the difference between the player's position and the center of the target.

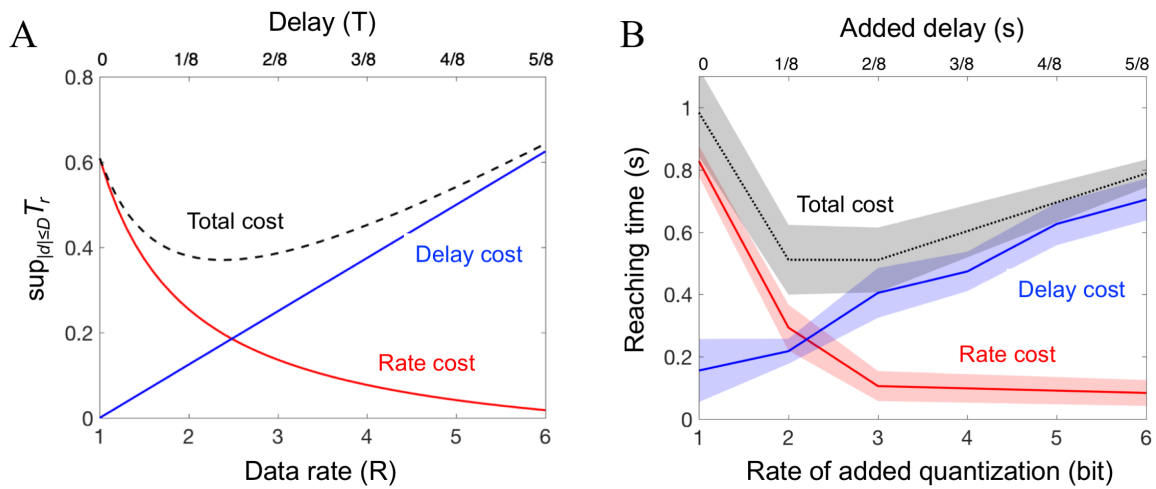


Figure 3: The SATs. (A) Theoretical SATs in the reaching task. The delay cost (blue line), rate cost (red line), and the total cost (dashed black line) in Eq. 5 are shown with varying component SAT  $T = (R - 1)/8$ . (B) Empirical SAT in the reaching task. Data obtained from 4 subjects who performed the task over a range of time delays and quantization (See Fig. S1 for data from individual subjects). The blue line shows the performance with added actuation delay  $T$ ; the red line shows the performance with added quantization of rate  $R$ ; and the black line shows the performance with added delay and quantization subject to the SAT  $T = (R - 1)/8$ . The shaded region around the lines is standard errors.

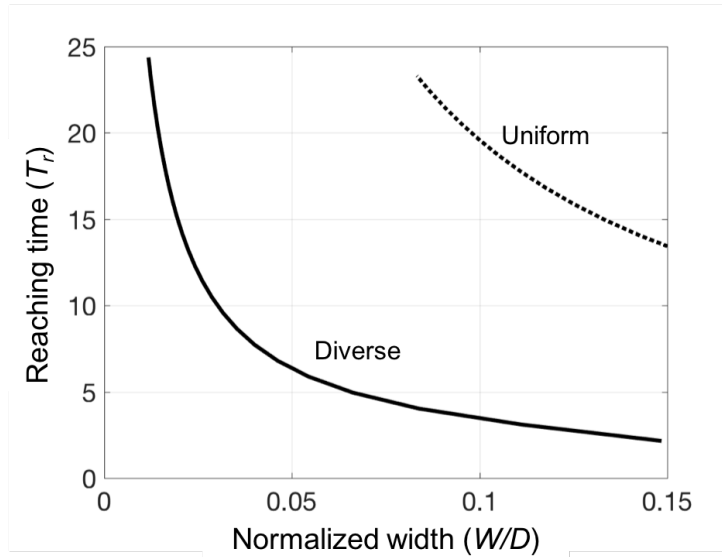
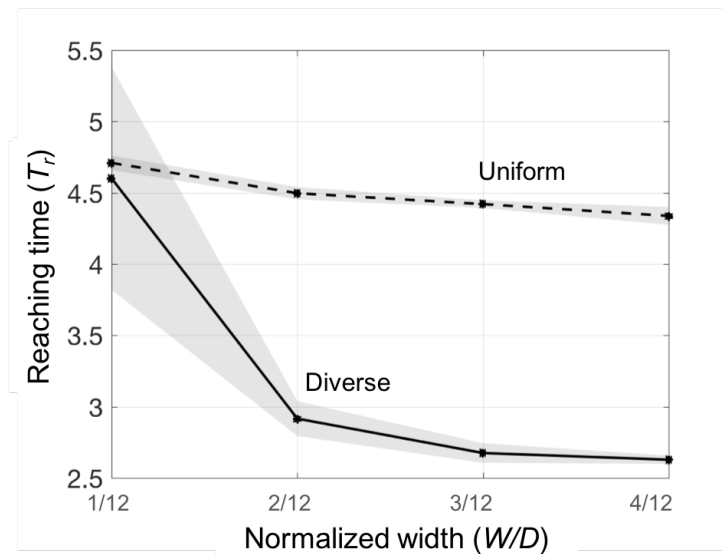
**A****B**

Figure 4: Experimental confirmation of predicted diversity advantage in reaching. (A) Theoretical DSSs in the reaching task derived from the SATs of a feedback loop implemented by a muscle composed of uniform (dashed line) or diverse motor units (solid line). The DSSs for two feedback loops with diverse muscles and uniform muscles are shown in FigS4. (B) Benefits from diversity in the reaching task. The plot shows the performance of a subject who performed the reaching task with uniform or diverse speeds, which is designed to mimic the case of uniform or diverse muscles, respectively. See the Supplementary Material for more detail.

## **Supplementary Material**

The nerve signaling SAT

The impact of nerve SATs on reaching SATs

The impact of muscle SATs on reaching SATs

Experimental setting

Diversity sweet spots in transportation

Figs. S1-S5

Table S1

Video S1

References and notes

## Supplementary Materials

### The nerve signaling SAT (Eq. 3 in the main text)

In this section, we characterize the SATs for neural signaling. The formula for the SATs depend on how the nerves encode information (*e.g.* spike-based, spike-rate, etc.). Here, we focus on spike-based encoding and present the discuss of alternative encoding strategies in our companion paper (30). In a spike-based encoding scheme, information is encoded in the presence or absence of a spike in specific time intervals, analogous to digital packet-switching networks (? , ?). This encoding method requires spikes to be generated with sufficient accuracy in timing, which has been experimentally verified in multiple types of neuron (? , ?). We consider a nerve with bundles of axons having average radius  $\rho$ . We use  $n$  to denote the number of axons in a nerve. We use  $T_s, R$  to denote the delay and data rate (*i.e.* the amount of information in bits that can be transmitted) of a nerve. When the signaling is precise and noiseless, an axon with achievable firing rate  $\phi$  can transmit  $\phi$  bits of information per unit time. For sufficiently large myelinated axons, we assume that the propagation speed  $1/T_s$  is proportional to the axon radius  $\rho$  (6), *i.e.*

$$T_s = \alpha/\rho \quad (1)$$

for some proportionality constant  $\alpha$ . We also model the achievable firing rate  $\phi$  to be proportional to the axon radius  $\rho$ , *i.e.*

$$\phi = \beta\rho, \quad (2)$$

for some proportionality constant  $\beta$ . Moreover, the space and metabolic costs of a nerve are proportional to its volume (6), and given a fixed nerve length, these costs are proportional to its total cross-sectional area  $s$ . Using the above properties, we have

$$R = n\phi = \frac{s}{\pi\rho^2}\beta\rho = \frac{s\beta}{\pi} \frac{1}{\rho} = \frac{s\beta}{\alpha\pi} T_s. \quad (3)$$

This leads to  $R = \lambda T_s$ , where  $\lambda = s\beta/\pi\alpha$  is proportional to the spatial and metabolic cost to build and maintain the nerves.

### The impact of nerve SATs on reaching SATs

We propose a control system model that captures the nerve SAT tradeoffs. Toward this end, we consider a reaching task in which the subject needs to move to a given target as quickly as possible. The target is chosen from a set of disjoint intervals of length  $W$  in a range of distance  $D$  from the origin, *i.e.*  $[-D, D]$ . We define the reaching time as

$$T_r = \{\tau : |x(t)| \leq W/2 \text{ for any } t \geq \tau, |x(0)| \leq D\}. \quad (4)$$

It can be observed that the range  $[-D, D]$  can hold no less than  $2D/W$  disjoint intervals of length  $W$ , so the amount of information required to differentiate one interval from other such intervals can be computed to be  $F = \log_2(2D/W)$  bits. This means that, after the target location is sensed,  $F/R$  time steps are required to deliver  $F$  bits of information from the sensors to the actuators. At each step, the information takes  $T$  time intervals to transmit. Therefore, the worst case reaching time cannot be smaller than the sum of the two types of delays,  $T + F/R$ , yielding Eq. 5 in the main text. A more detailed description of the math tools applicable to a more general setting can be found in our companion paper (30).

As suggested by the existing literature, in the setting described in this paper,  $F$  quantifies the amount of information required to perform the reaching task in the required accuracy. See (? , 8, 20, 23, 24) and references therein for more details on how  $F$  and related quantities are associated with the required information for other similar (stochastic) settings. Moreover, the above proof provide insights into Fitts' law, *i.e.*  $T_r = p + qF$ , and how the nerve signaling SATs impact the reaching SATs:  $p = T$  is determined from the delay in reacting and transmitting the target information, and  $q = 1/R$  is determined from the limited data rate in the feedback loop.

## The impact of muscle SATs on reaching SATs

Existing literature has studied Fitts' law using conventional control theory that does not account for explicit hardware constraints. For example, conventional control theory can model jerk (?), smoothness (?), acceleration (?), and kinematics (?), among others. Although quantities like jerk may be reduced as a result of optimizing control performance subject to hardware constraints, they are unlikely to be the ultimate target of optimization. In order to connect the hardware and reaching SATs, we propose a control system model that captures the muscle SAT tradeoffs explicitly. Toward this end, we use a simplified muscle model that includes  $m$  motor units. Each motor unit is indexed by  $i \in \{1, 2, \dots, m\}$  and is associated with a reaction speed and a strength level. We use  $F_i$  to denote its strength and assume without loss of generality that  $F_1 \leq F_2 \leq \dots \leq F_m$ . Recall from the main text that the muscle SAT can be quantified using the following formula:

$$\begin{aligned} \frac{d}{dt}a_i(t) &= \alpha f_i^p (1 - a_i(t)) - \beta a_i(t) \\ a_i^q(t) &= c_i(t) \end{aligned} \quad (5)$$

where  $\alpha = 1, \beta = 1, p = 1, q = 3, f_i = 1/((1/F_i)^{1/q} - 1)$  are fixed constants (17). See Fig. S2 for an illustration of the dynamics of Eq. 5. If a motor unit is recruited at time  $t = 0$ , then its strength  $c_i(t)$  rises according to Eq. 5 and  $c_i(t) = 1(t)F_i$  as follows:

$$c_i(t) = \left\{ \frac{f}{f+1} (-e^{-t(f+1)} + 1) \right\}^{1/q} \quad (6)$$

where  $1(t)$  is a unit step function. Similarly, when a recruited motor unit is released at time  $t = 0$ , its contraction rate falls according to Eq. 5 with  $f_i(t) = 1(-t)/((1/F_i)^{1/q} - 1)$  as

follows:

$$c_i(t) = c_i(0)e^{-t}. \quad (7)$$

Next, we consider using the muscle to perform a reaching task. The control process in reaching is modeled by Eq 1-2 in the main text. Recall that  $x(t)$  is defined as the error between the actual position and the target (desired) position. Given a static target, the error dynamics only depends on the dynamics of the actual position. So, we have

$$\frac{d^2}{dt^2}x(t) = \sum_i c_i(t) - h(t) \quad (8)$$

where the sum is taken over all recruited motor units. The function  $h(t)$ , which captures the friction acting against the motion, takes the form

$$h(t) = \begin{cases} h_s & \text{if } dx(t)/dt = 0 \\ h_k & \text{otherwise,} \end{cases} \quad (9)$$

where  $h_s$  can be obtain from the coefficient of static friction, and  $h_k$  from the kinetic friction.

To study the benefit of diversity in motor units, we consider two cases: having two mid-sized motor units (denote as the uniform case), having a large motor unit and a small one (denote as the diverse case). In both cases, the total resource use (total cross-sectional area of all motor units) is set to be equivalent, and so does the sum of strength levels for both cases. Fig. S3 (A) shows the achievable reaching time and distance as dots when each motor unit contracts for periods of length ranging from 0.75 to 14.75 with 0.5 increment. This increment in duration captures the latency and limitations on timing precision in reaction. The uniform muscle case has two motor units with the same strength level ( $F_1 = F_2 = 0.5$ ), and the diverse case has two motor units with different strength levels ( $F_1 = 0.85, F_2 = 0.15$ ). In the diverse case, Fig. S3 (B) zooms in the plots in Fig. S3 (A) and compares the achievable reaching times between the uniform cases and diverse cases when the contraction duration is set to be equal. From Fig. S3 (A)-(B), we can observe that having diverse motor units is beneficial. Compared with the uniform case, large motor units in the diverse case are helpful for reaching longer distance due to fast activation, while the small motor units can be used to achieve precise movements. This benefit of reaching SATs is shown in Fig4A of the main text.

To study the benefit of diversity in muscles, we consider two cases: having two muscles with the same strength level (denote as the uniform case), having two muscles with different strength levels (denote as the diverse case). The total strength for each case is set to be the same, so the total cross-sectional area used by the muscles in each case is also equivalent. Fig. S4 compares the reaching SATs for each case. Similarly, having diverse muscles is beneficial because the muscle with larger strength in the diverse case is helpful for achieving faster activation, and the muscle with smaller strength is helpful for achieving precise movements.

## Experimental settings

To verify the theoretical prediction, we conducted a reaching task experiment under different externally added visual input delay and actuation quantization. Subjects are asked to steer a wheel to reach (and stay) in the target gray zone as quickly as possible. To test the effect of having a delay and limited data rate in the feedback loop, we conducted two types of experiments: 1) reaching with added delay, 2) reaching with added quantization. In 1) reaching with added delay, the visual display was delayed for  $0, 1/8, \dots, 5/8$  seconds. In 2) reaching with added quantization, we quantized the wheel input by  $1, 2, \dots, 6$  bits per unit sampling interval, where the sampling interval is set to be  $350ms$ . Specifically, a quantizer of data rate  $R$  is implemented as follows: after  $n$  sampling intervals, the gray zone is centered at the target position with a width of the screen length times  $2^{-nR}$ . This intends to simulate the process of sending  $R$  bits per sampling interval and estimating the target with an error of size  $2^{-nR}$  after  $n$  sampling intervals (see the implementation of limited data rate in Supplementary video S1). We tested 50 trials for each setting and measured the reaching time. The subject-specific internal delay was estimated for each subject by the minimal time to reach the target area with no external delay and with the maximum rate (mean = 1.17s, SD = 0.06). The internal delay was subtracted for the following analysis. Plots of the mean movement time from single subjects are shown in Fig. S1, and the average of all four subjects is shown in Fig. 3B in the main text. The blue and red line in each plot shows the result from case 1) and case 2) respectively. The dashed line in each plot shows the sum of total error from case 1) and case 2) with the SAT constraint  $T = (R - 1)/8$ .

To test the effects of diversity in actuation on system performance with the experiment, we set the target distance to be  $D = 12$  and varied the target width to be  $W = 1, 2, 3, 4$ , similar to the simulation of Fig S3. We considered two cases: when the subject only has one choice of speed ( $|V_0| = 2.5$ ), and when the subject can choose two speeds ( $|V_0| = 2.5$  and  $|V_1| = 5$ ). Specifically, in the uniform case, the speed is set to be  $V = -2.5$  when the subject steers to the left side (angle from the middle  $\leq 0^\circ$ ), and  $V = 2.5$  when the subject steers to the right side (angle from the middle  $> 0^\circ$ ). In the diverse case, the speed is set to be  $V = -2.5$  when the subject gently steers to the left side ( $-30^\circ < \text{angle from the middle} \leq 0^\circ$ ), and  $V = -5$  when the subject further steers to the left (angle from the middle  $\leq -30^\circ$ ). The right side is similar. Here, the speed is controlled by the wheel angle. The unit of the speed is a screen unit per sampling intervals, where a screen unit is set so that the total size of 1000 units sum up to equal the whole screen monitor (15 inches with  $1920 \times 1080$  resolution), and a sampling interval is set to be 0.01 seconds. The performance from both cases is shown in Fig. 4B. The diverse case performs much better than the uniform case because subjects in the uniform case can only use the lower speed to satisfy the required accuracy, whereas subjects in the diverse case can achieve better reaching SATs by starting with the higher speed to reach the target quickly and then switching to the lower speed to stay inside the desired zone.

Similar phenomenon can also be observed in transportation. We consider the setting of traveling from one location to another using certain means of transportation. We assume that

the means of transportation used has fast enough acceleration such that the velocity can be modeled by a pulse function. We consider case when only one means of transportation can be used (denote as the uniform case) and when diverse means of transportation can be used (denote as the diverse case). In the diverse case, there is a time loss when switching between different means of transportation. Fig S5 compares the travel time and required accuracy for the diverse and uniform cases. The diverse case performs much better than the uniform case because diverse case can exploit faster means of transportation to travel quickly while use the slower means of transportation to achieve the required accuracy.

## Diversity sweet spots in transportation

Diversity sweet spots can be observed in transportation as well. Let us first consider a simple transportation model: traveling by walking, driving, or flying. We index these means of transportation by  $i = 1, 2, 3$  respectively and use  $s_i$  to denote their speed and  $e_i$  to denote their resolution. As walking is typically slower than driving, and driving is slower and flying, we assume that  $s_1 < s_2 < s_3$ . Meanwhile, as flights can only land on airports, cars can only stop at parking lots, and a walker can stop at almost anywhere, we assume that  $e_1 < e_2 < e_3$ . Let  $T_E(D)$  be the time to travel distance  $D$  with tolerable error  $E$ , where  $E$  satisfies  $E \ll D$  and  $E \geq r_1$ . When the traveler is only allowed to use a single means of transportation, the relation between the traveling time  $T_E(D)$  and accuracy constraint  $E$  follows

$$T_E(D) = \begin{cases} D/s_1 + O(1) & \text{if } e_1 \leq E \leq e_2 \\ D/s_2 + O(1) & \text{if } e_2 \leq E \leq e_3 \\ D/s_3 + O(1) & \text{if } e_3 \leq E, \end{cases} \quad (10)$$

where  $O(1)$  represents the terms that do not scale with  $D$  as  $D \rightarrow \infty$ . On the other hand, when the traveler is allowed to combine three means of transportation, the traveling time  $T$  and resolution  $E$  is given by

$$T = D/s_3 + O(1). \quad (11)$$

This suggests that, as  $D \rightarrow \infty$ , the flexibility to combine walking, driving, and flying enables the traveling time to scale according to the fastest means of transportation.

## References and Notes

1. E. Todorov, M. I. Jordan, *Nature neuroscience* **5**, 1226 (2002).
2. A. J. Nagengast, D. A. Braun, D. M. Wolpert, *Journal of neurophysiology* **105**, 2668 (2011).
3. D. W. Franklin, D. M. Wolpert, *Neuron* **72**, 425 (2011).

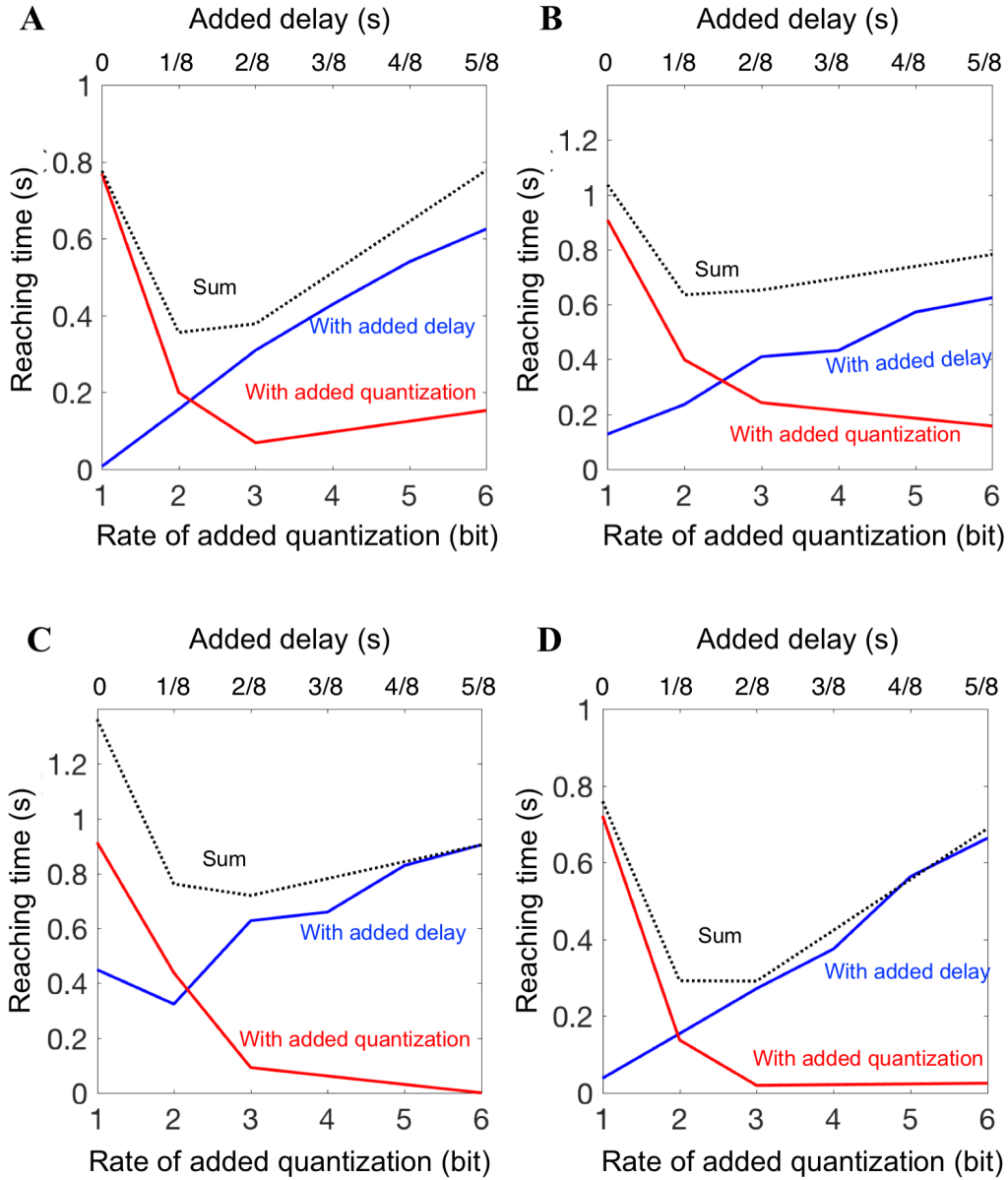
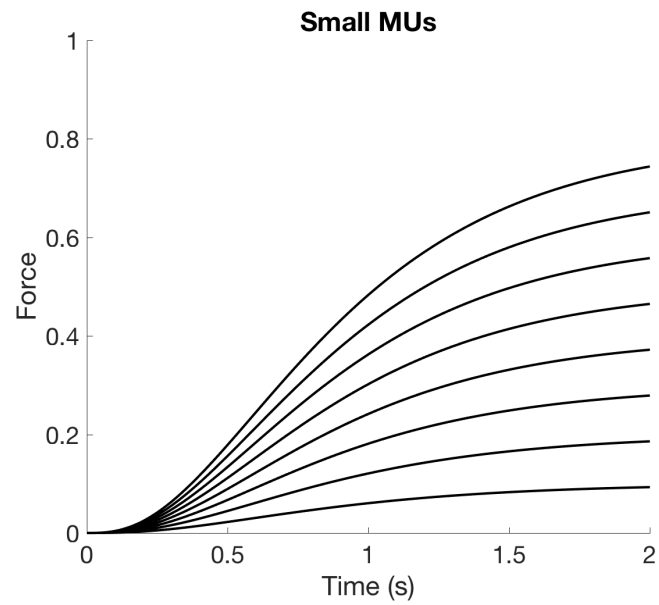


Figure S1: Empirical SATs in the reaching task. The blue lines show the reaching time with added delay; the red lines show the reaching time with added quantization; and the black lines show the sum of the two subject to  $T = (R - 1)/8$ .

**A**



**B**

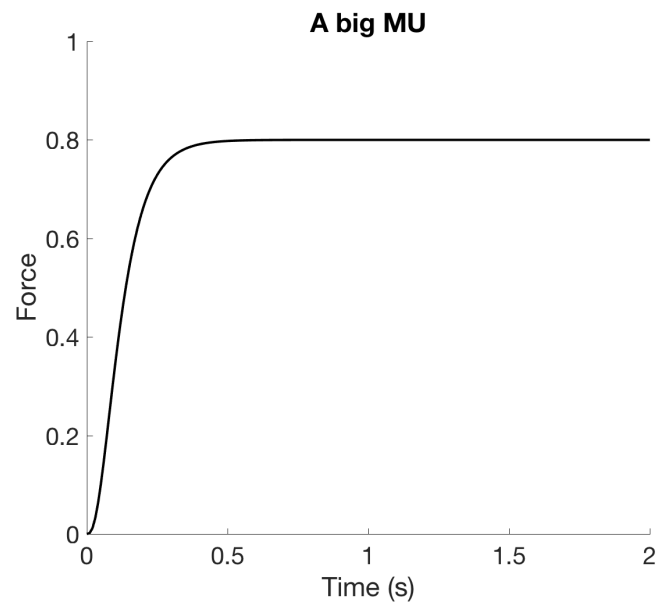


Figure S2: Explanation for component-level speed-accuracy trade-offs (SATs) in muscles. The dashed lines show the individual and cumulative response of the motor units, generated according to Eq. (6). (A) The response of having 8 small motor units of strength level 0.1. (B) The response of having one large motor unit of strength level 0.8. The total strength of all motor units for (A) and (B) are set to be same.

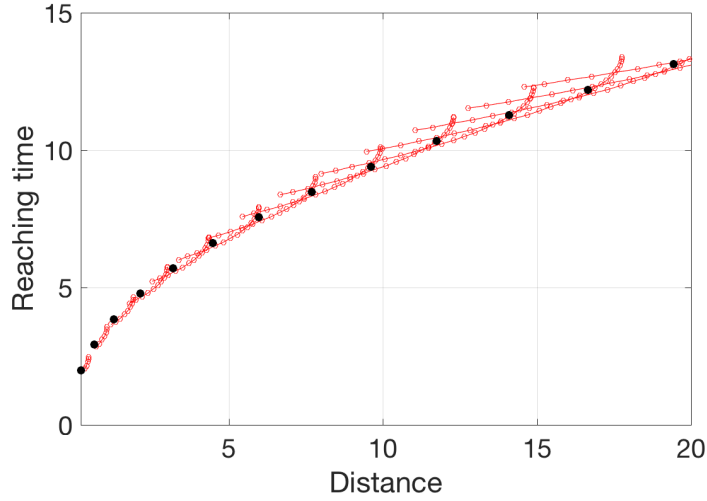
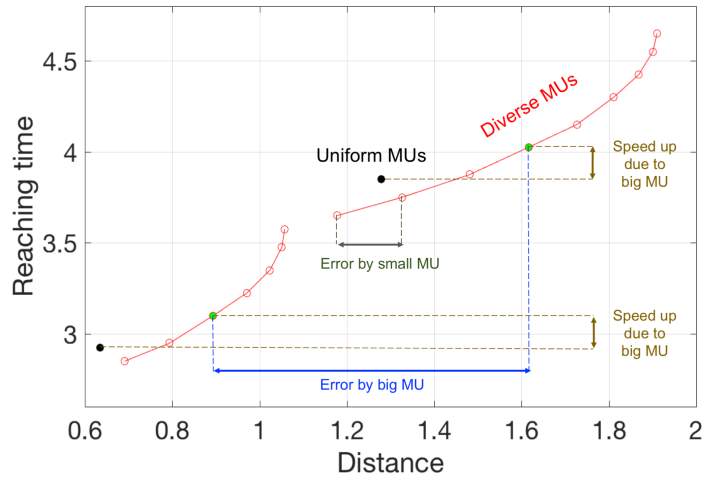
**A****B**

Figure S3: Achievable reaching distance and reaching time. The uniform case has two motor units with the same strength ( $F_1 = F_2 = 0.5$ ), and the diverse case has two motor units with different strengths ( $F_1 = 0.85, F_2 = 0.15$ ). The sum of the strength of all motor units is set to be same for both cases. The muscle contraction duration for each motor unit ranges from 0.75 to 14.75 with 0.5 increment. The friction parameters are set to be  $h_s = 0.6$  and  $h_k = 0.54$ . Each dot represents an achievable pair between the reaching distance and time in uniform case (black) and diverse case (red). (A) Original plot. (B) Zoomed plot. The green dot represents the achievable pair when the contraction duration of both motor units is set to be equal in the diverse case.

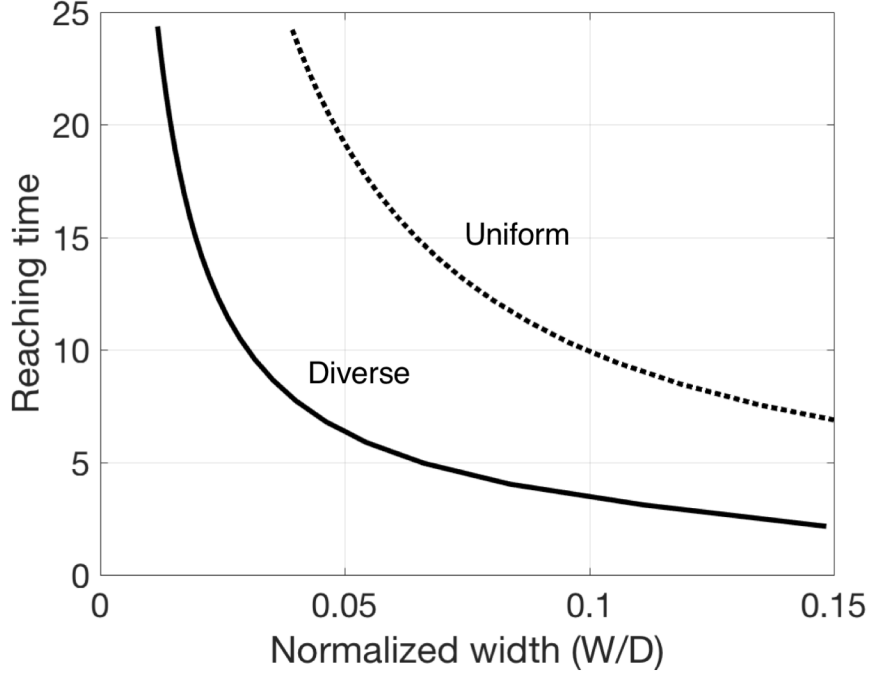


Figure S4: Reaching SATs when uniform or diverse muscles are used. The uniform case has two muscles with the same strength ( $F_1 = F_2 = 0.5$ ), and the diverse case has two muscles with different strengths ( $F_1 = 0.85$ ,  $F_2 = 0.15$ ). The sum of the strength of all muscles is set to be the same for both cases. The friction parameters are set to be  $h_s = 0.6$  and  $h_k = 0.54$ .

Parameter	Description
$x(t)$	Error at time step $t$
$\mathcal{K}$	Controller
$T_s \geq 0$	Signaling delay
$T_i \geq 0$	Internal delay
$T = T_s + T_i$	Total delay
$T_t$	Time to reach target
$R$	Information rate (bits per unit time)
$\lambda$	Cost associated with the resource use

Table S1: Parameters in the basic model.

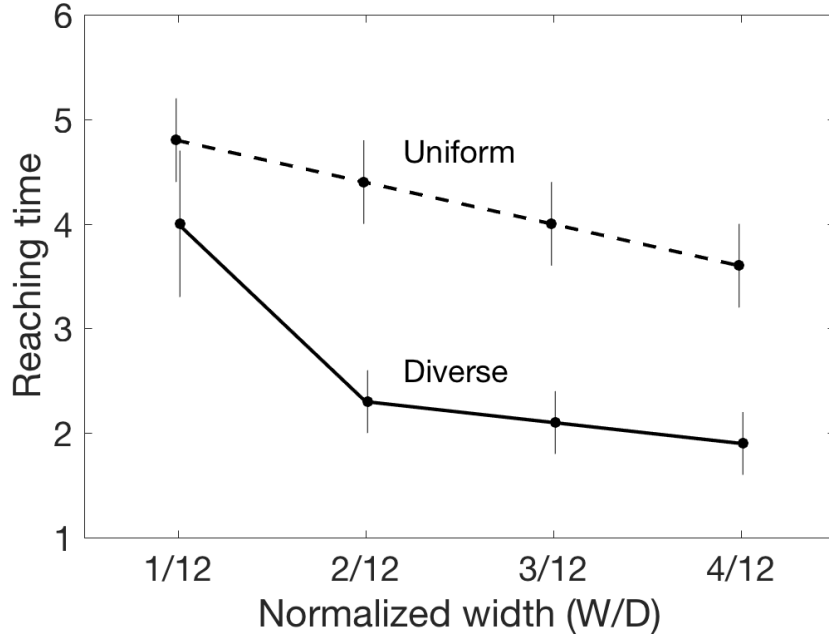


Figure S5: Reaching time versus accuracy constraints. We consider the setting of traveling distance  $D = 12$  with an accuracy requirement ranging  $W = 1, 2, \dots, 4$ . There are two means of transportation: one has a speed of 2.5 with resolution 1, the other has a speed of 5 with resolution 1.5. We consider two cases: when only one means of transportation can be used (denote as the uniform case) and when diverse means of transportation can be used (denote as the diverse case). In the diverse case, the time loss in switching between different means of transportation is 1. In the uniform case, only  $v = 1, e = 1$  can meet the requirement of the task with  $W = 1$ . The error bar illustrates the upper lower bounds of the reaching time.

4. S. Lac, J. L. Raymond, T. J. Sejnowski, S. G. Lisberger, *Annual review of neuroscience* **18**, 409 (1995).
5. S. G. Lisberger, *Neuron* **66**, 477 (2010).
6. P. Sterling, S. Laughlin, *Principles of neural design* (MIT Press, 2015).
7. P. M. Fitts, J. R. Peterson, *Journal of experimental psychology* **67**, 103 (1964).
8. Fitts's law (wikipedia).
9. A summary of the parameters used is given in **Table S1**.
10. J. A. Perge, J. E. Niven, E. Mugnaini, V. Balasubramanian, P. Sterling, *Journal of Neuroscience* **32**, 626 (2012).
11. J. Stenum, *Journal of Experimental Biology* **221**, jeb170233 (2018).
12. H. L. More, *et al.*, *Journal of Experimental Biology* **216**, 1003 (2013).
13. H. L. More, *et al.*, *Proceedings of the Royal Society B: Biological Sciences* **277**, 3563 (2010).
14. Bigger animals have more inertia and can tolerate longer delays. they also use more time to compute in part because large animals (elephants, etc.) are more prone to falling.
15. E. Henneman, G. Somjen, D. O. Carpenter, *Journal of neurophysiology* **28**, 560 (1965).
16. G. Goldspink, *Journal of experimental biology* **115**, 375 (1985).
17. V. Brezina, I. V. Orekhova, K. R. Weiss, *Journal of neurophysiology* **83**, 207 (2000).
18. In other words, the time required for a muscle to reach to  $c_i(t) = f_i$  from  $c_i(0) = 0$  is decreasing in  $f_i$ .
19. The Kronecker delta function is defined as follows:  $\delta(t) = 1$  if  $t = 0$ , and  $\delta(t) = 0$  otherwise.
20. P. M. Fitts, *Journal of experimental psychology* **47**, 381 (1954).
21. A. Hodgkin, *The Journal of physiology* **125**, 221 (1954).
22. D. Hartline, D. Colman, *Current Biology* **17**, R29 (2007).
23. T. O. Kvåiseth, *Perceptual and Motor Skills* **49**, 291 (1979).
24. I. S. MacKenzie, *Journal of motor behavior* **21**, 323 (1989).

25. H. Hatze, *Bulletin of mathematical biology* **41**, 407 (1979).
26. These laws include the weber-fechner law, a log relation between the physical change in a stimulus and the perceived change in human perception; the ricco law for visual target detection for unresolved targets; the accot-zhai law for steering, a generalization of fitts' law for 2d environments; the spacing effect of ebbinghaus for long-term recall from memory; and the hick-hyman law for the logarithmic increase in the time it takes to make a decision as the number of choices increases.
27. D. Kahneman, P. Egan, *Thinking, fast and slow*, vol. 1 (Farrar, Straus and Giroux New York, 2011).
28. N. R. Franks, A. Dornhaus, J. P. Fitzsimmons, M. Stevens, *Proceedings of the Royal Society of London. Series B: Biological Sciences* **270**, 2457 (2003).
29. L. Chittka, P. Skorupski, N. E. Raine, *Trends in ecology & evolution* **24**, 400 (2009).
30. Y. Nakahira, et. al, Diversity sweet spots in layered architectures and speed-accuracy trade-offs in sensorimotor control. Unpublished.